Commun. Comput. Phys.
doi: 10.4208/cicp.401011.220212s

Vol. **13**, No. 3, pp. 629-648
March 2013

Extended BGK Boltzmann for Dense Gases

Saikishan Suryanarayanan, Shiwani Singh and Santosh Ansumali*

Engineering Mechanics Unit, Jawaharlal Nehru Centre for Advanced Scientific Research, Jakkur, Bangalore 560064, India.

Received 31 October 2011; Accepted (in revised version) 22 February 2012

Available online 29 August 2012

Abstract. An alternate BGK type formulation of the Enskog equation has been recently proposed [1]. It was shown that the new model has a valid H-theorem and correct thermal conductivity. We propose Lattice Boltzmann (LB) formulation of this new Enskog-BGK model. The molecular nature of the model is verified in case of shear flow by comparing the predicted normal stress behavior by the current model with the prediction of molecular dynamics simulations. We extend the model for multiphase flow by incorporating attractive part as Vlasov type force. To validate multiphase formulation, the results of 3D simulations of a condensing bubble in a periodic box are presented.

AMS subject classifications: 76T10, 82C40

Key words: Lattice Boltzmann method, multiphase flow, Enskog equation.

1 Introduction

The Lattice Boltzmann Method (LBM) has emerged as an viable alternative to more mature methods such as Discrete simulation Monte Carlo (DSMC) for studying rarefied gas flow in the regime of moderate to low Knudsen number $(\mathrm{Kn} < 1)$ and low Mach number limits $(\mathrm{Ma} \ll 1)$ [2–8]. Apart from efficient discretization, the important feature which makes the method very efficient is the use of simplified collision mechanism known as the Bhatnagar-Gross-Krook (BGK) collision approximation [9–12]. While BGK-LBM is an excellent tool for studying dilute gases even at the molecular level [2], the success of the method for dense gas is at best very modest. While a top-down connection from continuum formulation of multiphase flow via diffuse interface theory is on firm ground [13, 14], despite good progress made in connecting these models with Enskog-Vlasov type theories [15–17], so far connection from microscopic theory is not so well settled. Perhaps one of the reason for this is formulating a consistent BGK type model

*Corresponding author. *Email addresses:* saikishan@jncasr.ac.in (S. Suryanarayanan), shiwani@jncasr.ac.in (S. Singh), ansumali@jncasr.ac.in (S. Ansumali)

for Enskog equation is non-trivial. There is no straightforward extension of BGK for dense gases or multiphase flows, as the equilibrium is still Maxwell-Boltzmann in velocity space but there is a non-ideal contribution to pressure.

The dense gas analog to the Boltzmann equation was given by Enskog [18] who introduced a short range pair correlation function in the collision integral. While the Enskog equation has a valid H-theorem, it is not convenient for simple numerical implementation. Therefore, a BGK type phenomenological model for dense gases can be very useful for simulation of multiphase flows. There have been several attempts to address this issues by expanding the Enskog collision integral around BGK collision term by a formal Hermite expansion [19–21]. The coefficients are then tuned to obtain correct conservation laws. While most of the present Multiphase LBM are based on this class of models, the lack of H-theorem and incorrect thermal conductivity behavior are some of the weakness of these approaches [13, 15, 17, 21, 22]. Recently, some of these issues were resolved in a BGK type formulation for the dense gas [1]. In the present work, we consider this recently proposed extension to the Boltzmann equation, wherein the effect of finite density is accounted at a mean field level by suitable generalization of the advection velocity, while retaining the point-particle based collision integral of the Boltzmann equation. This model has both correct conservation laws as well as a valid H-theorem [1].

We explain the physical motivation of the model and conservation laws in Section 2. In Section 3, we compare the analytical solution of the present model in uniform shear flow (USF) with Molecular Dynamics (MD) to validate its molecular nature. We introduce the model in a discrete velocity lattice in Section 4, following which we extend it to multiphase flows by addition of attractive term in Section 5. We introduce the LB scheme with space and time discretization and discuss the various approximations that are essential to retain the numerical efficiency of BGK-LBM in Section 6. We present results from 1D simulation, including comparison with Maxwell construction in Section 7. Section 8 deals with extension to 3D and results of simulations of a condensing bubble in D3Q27 are presented.

2 Present model

In this section, we will review main features of the modified BGK type of approach for Enskog dynamics as presented in [1]. As compared to Enskog, this model takes an alternate approach to account for the effect of finite density by the generalization of the advection velocity. The physical motivation behind the modification of the advection velocity as opposed to collision is that the effect of the collective motion on the tagged particles will manifest itself as a modification of mean-free path concept. Thus, in this model the evolution equation for the one particle distribution function $f(\mathbf{x},\mathbf{v},t)$ with BGK collision model is given as

$$\frac{\partial f}{\partial t}+\frac{\partial}{\partial x_\alpha}(\hat{v}_\alpha f)+\frac{F_\alpha}{m}\frac{\partial f}{\partial v_\alpha}=\frac{f^{\mathrm{eq}}-f}{\tau}, \tag{2.1}$$

where $\hat{v}_\alpha$ is the modified advection velocity, $\mathbf{F}$ is either an external or internal Vlasov type force, m is the mass of the particle and τ is the relaxation time. By f^{eq}, we denote the Maxwell-Boltzmann equilibrium distribution. For the present discussion, we consider $\mathbf{F}=\mathbf{0}$ (until attractive force is introduced in Section 5).

The modified advection velocity written in its simplest form (sufficient to account for non-ideal part of the pressure) in terms of the compressibility factor $\chi^{\text{h}}=p/(\rho T)-1$ is

$$\hat{v}_\alpha = v_\alpha + \chi^{\text{h}}(v_\alpha - u_\alpha), \tag{2.2}$$

where the compressibility factor χ^{h} is a thermodynamic information to be known from molecular dynamics or other molecular considerations (similar to pair-correlation in Enskog description) and u_α is the mean fluid velocity. Note that we work with units in which $k_{\text{B}}/m=1$ (where k_{B} is the Boltzmann constant).

In order to obtain a physical understanding of Eq. (2.2), consider the leading order term as a first order approximation to the following model differential equation,

$$\frac{dv_\alpha}{dt} = \frac{\chi^{\text{h}}(\rho)}{\tau}(v_\alpha - u_\alpha), \tag{2.3}$$

which represents the change in the advection velocity due to finite density effects. This change should depend on the peculiar velocity, $\mathbf{v}-\mathbf{u}$ and χ^{h} contains the density dependence. The relaxation time τ is the only relevant timescale and hence is used to make the equation dimensionally consistent. It can be seen that the effect of this modification is to increase the velocity of any tagged particles traveling faster than the mean velocity and to slow down those that are already moving slower than the average and thus preventing 'jamming' in a mean-field sense. This permits effect of particle size to be accounted for at a mean-field level while still dealing with point-particles. This is illustrated in Fig. 1. Unlike earlier approaches, (the continuous form of) this model has a valid H-theorem (see Appendix A). We also like to note that the model presented by Ihle and Kroll [17] has some similarities to the present formulation but lacks H-theorem (details provided in Appendix A).

In order to see hydrodynamic behavior of the present model, we write evolution equation for the hydrodynamic fields, namely mass density ρ, momentum density j and temperature T, defined in terms of the one particle distribution function f as

$$\int f\{1, v_\alpha, \frac{v^2}{2}\}dv = \{\rho, j_\alpha, E\}, \tag{2.4}$$

with the energy of hard sphere as

$$E = \frac{j^2}{2\rho} + \frac{\rho DT}{2}, \tag{2.5}$$

the total heat flux is defined as

$$q_\alpha = (1+\chi^{\text{h}})\int f d\mathbf{v}(v_\alpha - u_\alpha)\left[\frac{(\mathbf{v}-\mathbf{u})^2}{2} - \left(\frac{D+2}{D}\right)T\right], \tag{2.6}$$

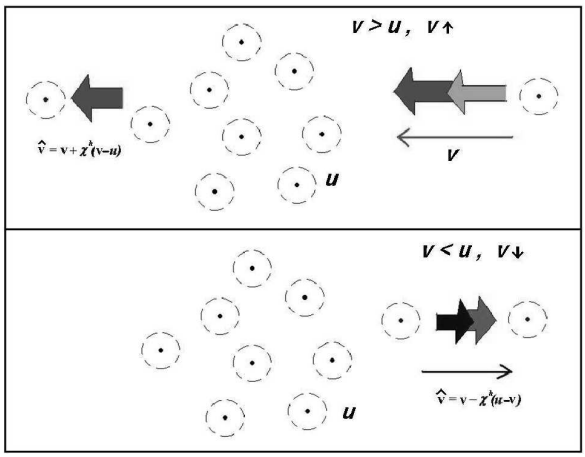

Figure 1: Illustration of physical motivation of the present model. Note that while it still uses point particles, it accounts for the effect of finite size (represented by the dotted circles) at a mean field level by accelerating faster particles and decelerating slower particles to prevent 'jamming'.

and the total stress tensor is defined as

$$\sigma_{\alpha\beta}=(1+\chi^{\mathrm{h}})\int f d\mathbf{v}\left[(v_\alpha-u_\alpha)(v_\beta-u_\beta)-\frac{1}{D}(\mathbf{v}-\mathbf{u})^2\delta_{\alpha\beta}\right], \tag{2.7}$$

where D is the dimension and the velocity is defined as $u_\alpha=j_\alpha/\rho$. Note that the heat flux and stress tensor defined above include both the kinetic and hard sphere contributions (for details refer [1]). Then the evolution equations for the moments are given as

$$\begin{aligned}&\partial_t\rho+\partial_\alpha j_\alpha=0,\\&\partial_i j_\gamma+\partial_\alpha(\rho u_\alpha u_\gamma+p\delta_{\alpha\gamma}+\sigma_{\alpha\gamma})=0,\\&\partial_t E+\partial_\alpha((E+p)u_\alpha+\sigma_{\alpha\gamma}u_\gamma+q_\alpha)=0,\end{aligned} \tag{2.8}$$

where pressure is given as

$$p=(1+\chi^{\mathrm{h}})\rho T, \tag{2.9}$$

and the closure relation for the stress tensor, $\boldsymbol{\sigma}$ and heat flux $\mathbf{q}$ can be obtained using Chapman-Enskog expansion [1] as

$$\sigma_{\alpha\gamma}=-\eta\left(\partial_\alpha u_\gamma+\partial_\gamma u_\alpha-\frac{2}{D}\partial_\beta u_\beta\delta_{\alpha\gamma}\right), \tag{2.10}$$

$$q_\alpha=-k\partial_\alpha T, \tag{2.11}$$

with dynamic viscosity $\eta=p\tau$ and thermal conductivity as $k=\tau pC_p$, with $C_p=(1+2/D)$ Based on the evolution equation for the hydrodynamic variables and stress tensor obtained using Chapman-Enskog expansion, we can say that at least in the domain where the hydrodynamic description is valid, the present model is expected to be a reasonable model. However, a more stringent test would be to analyze the behavior of the model for the microscopic flow and compare its performance with that of molecular dynamics.

3 Comparison with molecular dynamics

In order to study the molecular nature of present model, we choose the typical set up of uniform shear flow, where the detailed result is available for Enskog equation [19, 20]. Following the procedure described in [23], we use Lee-Edwards boundary condition [24]. This boundary condition is applied by transformation to the local rest frame of the fluid in which the proposed model admits a spatially homogeneous solution, corresponding to the USF with velocity gradient tensor given as $a_{\beta\alpha}=a\delta_{\beta x}\delta_{\alpha y}$, where a is the constant shear rate. The required transformation for the velocity as well as the space variable $\mathbf{x}$ in shear flow $u_\alpha=a_{\alpha\beta}x_\beta$ is

$$v'_\alpha=v_\alpha-a_{\alpha\beta}x_\beta,\qquad x'_\alpha=x_\alpha-a_{\alpha\beta}x_\beta t. \tag{3.1}$$

Under these transformations, the spatial derivative operator transforms as

$$\frac{\partial}{\partial x_\alpha}=(\delta_{\alpha\beta}-a_{\alpha\beta})\frac{\partial}{\partial x'_\beta}-a_{\beta\alpha}\frac{\partial}{\partial v'_\beta}. \tag{3.2}$$

Using Eqs. (3.1) and (3.2), the present model (Eqs. (2.1), (2.2)) for hard sphere is transformed as

$$\frac{\partial f}{\partial t}+(\delta_{\alpha\beta}-a_{\alpha\beta})\frac{\partial}{\partial x_{\beta'}}\left((1+\chi^{\rm h})v'_\alpha f\right)-a_{\beta\alpha}\frac{\partial}{\partial v'_\beta}\left((1+\chi^{\rm h})v'_\alpha f\right)=\frac{f^{\rm eq}-f}{\tau}. \tag{3.3}$$

Since, the system is completely homogeneous in local rest frame, Eq. (3.3) can be further simplified to obtain

$$\frac{\partial f}{\partial t}-a\frac{\partial}{\partial v'_x}\left((1+\chi^{\rm h})v'_y f\right)=\frac{f^{\rm eq}-f}{\tau}. \tag{3.4}$$

We define the second moments in the transformed co-ordinates as

$$P'_{xy}=\int v'_x v'_y f d\mathbf{v}',\qquad P'=\int (v'^2_x+v'^2_y)f d\mathbf{v}',\qquad N'=\int (v'^2_x-v'^2_y)f d\mathbf{v}', \tag{3.5}$$

we arrive at

$$P'_{xy}=-\rho a\tau(1+\chi^{\rm h})T,\qquad N'=2\rho a^2\tau^2(1+\chi^{\rm h})^2T. \tag{3.6}$$

We evaluate $(1+\chi^{\rm h})$ using Carnahan-Staring approximation [25] and choose τ corresponding to revised Enskog theory (RET) viscosity. In order to verify the molecular nature of the present model, variation of the normal stress with shear rate is compared with non-equilibrium Molecular dynamics (MD) simulations [26] for moderate ρ=0.5. As shown in Fig. 2, we get a good agreement MD simulation. It can be safely concluded that this model is capable of predicting the transport properties for a system of hard spheres far from equilibrium to a good extent. As it can be seen from Fig. 2, at high shear rates (0.7), present scheme is able to predict the normal stress within 24% of MD value while perturbative Enskog [26] leads to an error of 83%.

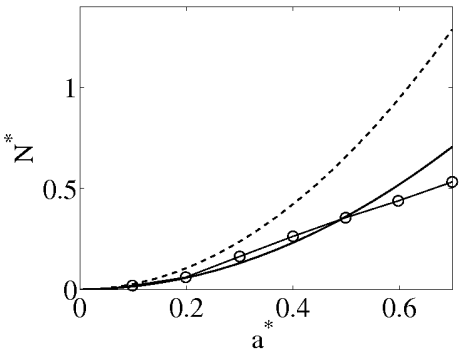

Figure 2: Reduced normal stress $N^* = (P^*_{xx} - P^*_{yy})$, where $P^*_{ij} = P_{ij}/\rho T$, as a function of reduced shear rate ($a^* = a/(4\rho\sqrt{\pi T})$ for $\rho = 0.5$, the perturbative calculation (dashed lines), MD simulation (circles) and present analysis (solid line).

4 Discrete velocity formulation

In this section, we would formulate a discrete velocity model for the current BGK formulation of Enskog type equation. We consider a set of discrete populations $f = \{f_i\}$ corresponding to the predefined discrete velocities $\mathbf{C}_i$ $(i = 1, \cdots, N)$ to represent the system. For this set of discrete populations, we define the moments as

$$\sum_i f_i \{1, C_{i\alpha}, C_{i\alpha}C_{i\beta}\} = \{\rho, \rho u_\alpha, \rho u_\alpha u_\beta + \rho T \delta_{\alpha\beta}\}. \tag{4.1}$$

The evolution equation for the discrete population is written in the BGK-form as

$$\partial_t f_i + C_{i\alpha}\partial_\alpha f_i + \partial_\alpha \left(\chi^{\mathrm{h}}(C_{i\alpha} - u_\alpha) f_i\right) = \frac{f_i^{\mathrm{eq}}(\rho, \mathbf{u}, T) - f}{\tau} + F_i, \tag{4.2}$$

where the external force term is written by using lowest order Hermite-projection of the gradient in the velocity space as

$$F_i = f_i^{\mathrm{eq}}(\rho, 0, T_0) \frac{F_\alpha C_{i\alpha}}{T_0}, \tag{4.3}$$

where T_0 is some reference temperature. Here we have assumed that the discrete velocity model under considerations is such that

$$\sum f_i^{\mathrm{eq}}(\rho, 0, T_0) C_{i\alpha} C_{i\beta} = \rho T_0 \delta_{\alpha\beta}. \tag{4.4}$$

The mean free time τ in the model is chosen in such a way that the viscosity expression matches density dependence as predicted by Enskog theory [18]. This implies

$$\tau = \frac{\tau_0}{1 + \chi^{\mathrm{h}}} \frac{\rho_0}{\rho} \left(1 + \rho b \left\{\frac{5}{8} + \rho b (0.2869 + \rho b (0.1103 + 0.0386 \rho b))\right\}\right), \tag{4.5}$$

where b is the parameter in the EOS that corresponds to the volume occupied by the molecules, ρ_0 and τ_0 are reference density and relaxation time respectively. In current work, we would be using Carnahan-Starling equation of state (CS-EOS) [25], which implies χ^{h} to be

$$\chi^{\mathrm{h}} = \frac{2\frac{\rho b}{4}(2-\frac{\rho b}{4})}{(1-\frac{\rho b}{4})^3}, \tag{4.6}$$

where in order to distinguish attractive and repulsive contributions in a general multiphase model, we have introduced superscript h for all hard-sphere repulsive contributions. For subsequent numerical implementations, we remind the reader that an alternate representation of the CS-EOS is often given in terms of chemical potential as

$$\mu^{\mathrm{h}} = T_0 \frac{8\frac{\rho b}{4}+3\left(\frac{\rho b}{4}\right)^2\left(\frac{\rho b}{4}-3\right)}{\left(1-\frac{\rho b}{4}\right)^3}. \tag{4.7}$$

We also like to note that the excess chemical potential μ^{h} is related to the non-ideal pressure contribution by the Gibbs-Duhem relation as

$$\partial_\alpha(\rho\chi^{\mathrm{h}}T_0) = \rho\partial_\alpha\mu^{\mathrm{h}}. \tag{4.8}$$

We shall demonstrate that using a formulation based on excess chemical potential is more efficient for numerical implementation in Section 6.

5 Multiphase model

In this section, we extend the present dense gas BGK model for multiphase flow. During phase transition, one expects the appearance of interfaces and hence additional terms that account for attractive force and surface tension are required in the chemical potential. We remind the reader here that surface tension at the gas-liquid interface is a result of density inhomogeneity which will manifest itself as the non-local term in the attractive part of the chemical potential. In terms of pressure, this would imply emergence of non-local contribution to the pressure tensor. We follow the typical convention used in the kinetic modeling approaches, where this effect is modeled as a Vlasov type model for the attractive force (see [27, 28] for detailed discussion).

This choice of force term in the discrete kinetic Eq. (4.2) would imply

$$F_\alpha = -\frac{\partial}{\partial x_\alpha}(\mu^{\mathrm{Att}}), \tag{5.1}$$

where μ^{Att}, the excess chemical potential due to the attractive contribution, is chosen to be of typical Van der Waals form. Here we remind the reader that the non-ideal (attractive) part of the pressure is related with the chemical potential as $\nabla P^{\mathrm{Att}} = \rho\nabla\mu^{\mathrm{Att}}$, due to the

Gibbs-Duhem relation. This is the reason that quadratic non-linearity of pressure implies linearity of chemical potential with respect to the density.

By writing the chemical potential in form of the mean-field approximation for the intermolecular potential $V(r)$ and by expanding density in Taylor's series, as elaborated in [15], we obtain the following expression,

$$\mu^{\text{Att}} = -2\hat{a}\rho - \kappa\nabla^2\rho, \tag{5.2}$$

where

$$\hat{a} = -\frac{1}{2}\int_{r<d_m} V(r)d\mathbf{r}, \tag{5.3}$$

$$\kappa = -\frac{1}{6}\int_{r<d_m} r^2 V(r)d\mathbf{r} \tag{5.4}$$

are assumed to be constants (d_m is the molecular diameter).

Further, $\hat{a}$ is related to the strength of the attractive term and depends on the critical temperature and the equation of state, while κ is a parameter related to surface tension [29]. It is convenient to represent it as $\kappa = \bar{\kappa}(d_m^2\hat{a})$ and $\bar{\kappa}$ is an empirical quantity of order 1.

The kinetic equation Eq. (4.2), along with force term chosen in Van der Waals form (Eqs. (5.1), (5.2)) is sufficient to describe liquid-gas phase transition. This can be seen by writing the momentum conservation using Eq. (4.2)

$$\partial_t(\rho u_\beta) + \partial_\alpha\left(p^{\text{ID}}\delta_{\alpha\beta} + \rho u_\alpha u_\beta + \sigma_{\alpha\beta}\right) + \partial_\beta p^E + \underbrace{\partial_\alpha(\kappa\partial_\beta\rho\partial_\alpha\rho)}_{\text{VdW}-\text{Stress}} = 0, \tag{5.5}$$

where $\sigma_{\alpha\beta}$ is given in Eq. (2.10), p^{ID} is the ideal part of pressure and the excess pressure p^E, is given as

$$p^E = \chi^{\text{h}}\rho T - \rho\hat{a}\kappa\Delta\rho - \frac{1}{2}\hat{a}\kappa|\nabla\rho|^2. \tag{5.6}$$

Thus this model correctly recovers the Van der Waals Stress [30](shown in underbrace in Eq. (5.5)), which confirms that it is capable of simulating liquid-gas phase transition.

6 Lattice Boltzmann implementation

We aim to derive the LB analog of the multiphase model (Eqs. (2.1), (2.2) and (5.2)), which can be written as

$$\partial_t f_i + C_{i\alpha}\partial_\alpha f_i = \frac{1}{\tau}(f_i^{\text{eq}} - f_i) + \Omega_i', \tag{6.1}$$

where

$$\Omega_i'(f) = \underbrace{-\partial_\alpha(\chi^{\text{h}}(C_{i\alpha} - u_\alpha)f_i)}_{F_i^h} \underbrace{-\frac{\rho W_i C_{i\alpha}}{T_0}\partial_\alpha(\mu^{\text{Att}})}_{F_i^{\text{Att}}}, \qquad W_i = f^{\text{eq}}(1,0,T_0). \tag{6.2}$$

Note that Ω_i has two contributions (shown with underbraces), namely the hard sphere contribution, F_i^h that arises from the correction to advection velocity and the attractive Vlasov force F_i^{Att}. The kinetic equation is integrated along the characteristic using trapezoidal rule, to obtain the evolution equation as

$$g(\mathbf{x}+\mathbf{C_i}\Delta t,t+\Delta t)=g(\mathbf{x},t)+2\beta\left(g_i^{\mathrm{eq}}-g_i\right)+2\beta\tau\Omega_i'(f), \tag{6.3}$$

where g is an auxiliary population defined as

$$g_i=f_i-\frac{\Delta t}{2\tau}(f_i^{\mathrm{eq}}-f_i)-\frac{\Delta t}{2}\Omega_i'(f), \tag{6.4}$$

with

$$\beta=\frac{\Delta t}{\Delta t+2\tau}. \tag{6.5}$$

After a set of straight forward calculations it can be shown that the lower order moments (namely density and velocity, on which isothermal equilibria depend) of distribution function f can be obtained from knowledge of moments calculated via auxiliary population g as

$$\rho(f)=\rho(g),\qquad u_\alpha(f)=u_\alpha(g)+\frac{1}{\rho}\sum_i\Omega_i'(f)C_{i\alpha}. \tag{6.6}$$

A minor rearrangement of this equation using Eq. (4.8), we can see that

$$u_\alpha(f)=u_\alpha(g)-\frac{\Delta t}{2}\partial_\alpha\mu+\frac{\Delta t}{2}\partial_\beta(\chi^{\mathrm{h}}\sigma_{\alpha\beta}), \tag{6.7}$$

where $\mu=\mu^{\mathrm{h}}+\mu^{\mathrm{Att}}$, which suggest that in the fully discrete picture velocity is getting three different kind of contributions: kinetic (via moment of g) contribution which leads to ideal gas behavior, a thermodynamic contribution (gradient of chemical potential), which leads to the non-ideal part of the pressure and third contribution which is non-equilibrium one. The non-equilibrium contribution is due to coupling between ideal and non-ideal part and is expected to be small. In subsequent numerical implementations, we will drop this term for the sake of simplicity.

In the absence of gradient of chemical potential term the standard discrete scheme for BGK-LBM is recovered which provides second order accuracy with a computational demand of a first order explicit scheme. For the current model, this advantage can be preserved, if in the discrete time stepper (Eq. (6.3)), we can replace $\Omega_i'(f)$ in terms of the auxiliary population g, via effective inversion of Eq. (6.4).

The explicit inversion of g in terms of f is possible if we can express Ω_i solely in terms of moments of g. In order to achieve such a representation, we consider the expansion of F_i^h in the Hermite basis around zero velocity equilibria and further using the fact that Mach number is small, repulsive contribution can be written solely in terms of the auxiliary population as

$$F_i^h\simeq-\partial_\alpha(W_iC_{i\alpha}\chi^{\mathrm{h}}\rho)-\underbrace{\frac{W_i\left(C_{i\alpha}C_{i\beta}-T_0\delta_{\alpha\beta}\right)\left[\partial_\alpha(\chi^{\mathrm{h}}\rho T_0u_\beta)+\partial_\beta(\chi^{\mathrm{h}}\rho T_0u_\alpha)\right]}{2T_0^2}}, \tag{6.8}$$

where the term represented by underbrace is the leading order term being ignored in the present work for sake of simplicity. Neglecting this term leads to a modification in viscosity and introduces a small error in Galilean invariance (shown in Appendix B). The above approximation allows us to write the discrete time stepper in closed form. We would like to mention here that these drastic simplifications are made to have a simple implementation and can be readily improved along the line of lattice Fokker Planck approach [31]. In this work, we would like to test the efficiency of the method even in presence of these drastic simplifications. The Chapman-Enskog expansion of the discrete model is presented in Appendix B to show the hydrodynamics simulated by the present scheme.

Finally, before we move to the actual numerical implementations, we would like to highlight a crucial numerical issue of breakdown of the Gibbs-Duhem equality in discrete case. As pointed out by earlier works [32, 33], in a typical discrete formulation, when the derivatives are approximated by finite differences, Eq. (4.8) may not hold

$$\partial_\alpha^{(D)}(\rho\chi^{\mathrm{h}}T_0) \neq \rho\partial_\alpha^{(D)}\mu^{\mathrm{h}}, \tag{6.9}$$

where $\partial^{(D)}$ is any appropriate finite difference operator. In such a scenario, one has to choose either pressure (that drives mechanical equilibrium) or chemical potential (that drives chemical equilibrium) as the basic quantity. We choose to formulate using chemical potential as we shall show that it leads to better accuracy. Let us consider a density profile $\rho = 1.5 + \tanh(20x)$. It can be observed from Fig. 3 that $\chi^{\mathrm{h}}\rho$ has a steeper variation than μ^{h} for CS-EOS. As a result it can be observed that a finite difference of μ^{h} is closer to the analytical solution than a finite difference of $\chi^{\mathrm{h}}\rho T_0$ for central difference scheme with same number of nodes. Hence we adopt the formulation based on excess chemical potential for the hard sphere contribution.

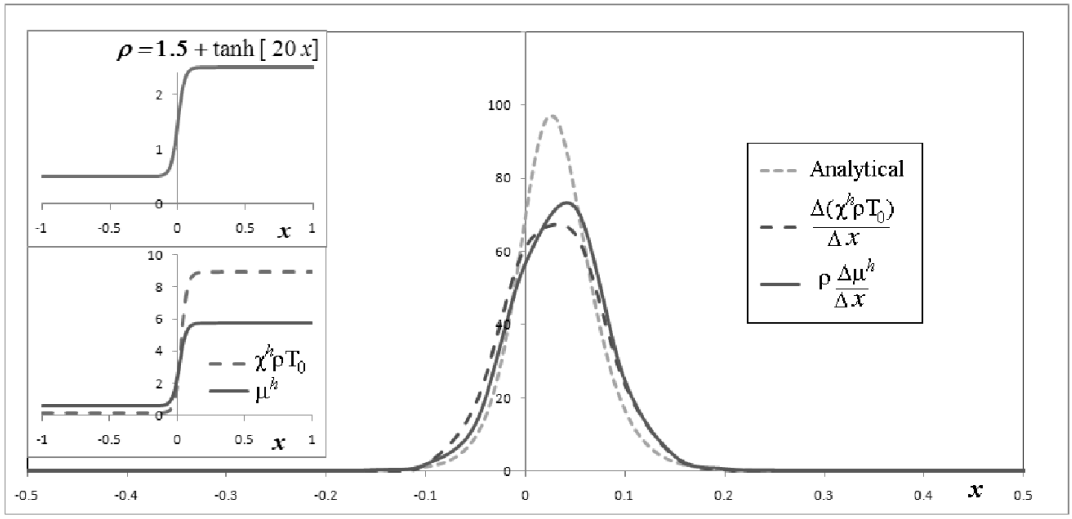

Figure 3: Illustration of discrete Gibbs Duhem inequality.

7 Numerical implementation in one dimension

We initially test the current discrete multiphase model in a 1D periodic setup. We choose the D1Q5 lattice [34], for which the set of lattice velocities and corresponding weights are given by

$$C_i = C\{-3,-1,0,1,3\}, \tag{7.1}$$

$$W_i = \frac{1}{720}\left\{16-5\sqrt{10},27(8-\sqrt{10}),64(4+\sqrt{10}),27(8-\sqrt{10}),16-5\sqrt{10}\right\}, \tag{7.2}$$

$$C = \sqrt{T_0\left(\frac{5}{3}+\frac{\sqrt{10}}{3}\right)}. \tag{7.3}$$

The equilibrium distribution is given by

$$f_i^{\mathrm{eq}} = W_i\rho\left[1+\frac{u_\alpha C_{i\alpha}}{T_0}+\frac{u_\alpha u_\beta}{2T_0^2}(C_{i\alpha}C_{i\beta}-T_0\delta_{\alpha\beta})+\frac{u_\alpha u_\beta u_\gamma}{6T_0^3}C_{i\gamma}(C_{i\alpha}C_{i\beta}-3T_0\delta_{\alpha\beta})\right]. \tag{7.4}$$

The discrete scheme for the current multiphase model in 1D are given by

$$g_i(x+C_{ix}\Delta t,t+\Delta t)-g_i(x,t) = 2\beta(g_i^{\mathrm{eq}}(\rho,u(f))-g_i)-2\beta\tau\rho\frac{W_iC_{ix}}{T_0}\partial_x\mu, \tag{7.5}$$

$$u_x(f) = u_x(g)-\frac{\Delta t}{2}\partial_x\mu. \tag{7.6}$$

All the spatial derivatives in Eqs. (7.5), (7.6) are computed using central difference in the present implementation. The corrected velocities given by Eq. (7.6) are used to evaluate g_i^{eq} in Eq. (7.5) before the collision step in the computation.

We initialize the populations using a uniform density perturbed with random disturbance and zero velocity. The random disturbance has an amplitude of 1% of the mean density and is drawn from a uniform probability distribution and march in time. A sample steady state solution is seen in Fig. 4. It can be observed that for $T < T_c$, there is separation into high density (liquid) and low density (gas) phases with smooth interfaces. Further, a good agreement between the observed density ratios and those predicted by Maxwell construction can be observed in Fig. 4, which also compares results obtained from a scheme that is based on χ^{h} instead of μ^{h}. Therefore, it can be safely concluded that exploiting the discrete Gibbs-Duhem inequality is essential for accuracy at higher density ratios.

8 Extension to 3D

In this section, we aim to simulate the present multiphase model in a 3D periodic box using D3Q27 lattice [35] for the same. The general scheme for time stepper and velocity

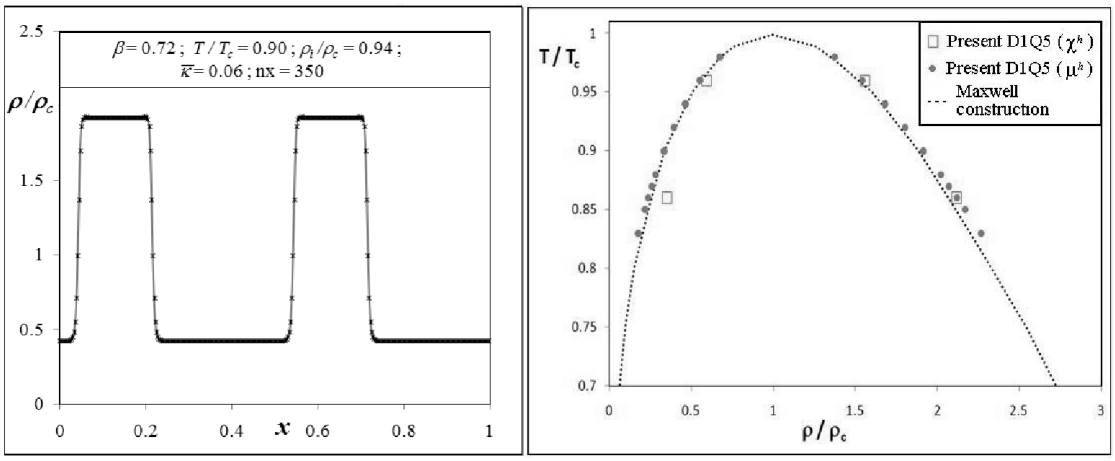

Figure 4: Results for D1Q5 Simulations.

correction for the present multiphase model is given by

$$g_i(\mathbf{x}+\mathbf{C}_i\Delta t,t+\Delta t)-g_i(\mathbf{x},t)=2\beta(g_i^{\mathrm{eq}}(\rho,u(\{f\}))-g_i)-2\beta\tau\rho\frac{W_iC_{i\alpha}}{T_0}\partial_\alpha\mu, \tag{8.1}$$

$$u_\alpha(f)=u_\alpha(g)-\frac{\Delta t}{2}\partial_\alpha\mu. \tag{8.2}$$

For preserving spherical symmetry in the discrete implementation in 3D, the gradients and Laplacian are computed in an isotropic fashion using the following:

$$\partial_\alpha G=\frac{1}{T_0\Delta t}\left(\sum W_iC_{i\alpha}G(\mathbf{x}+\mathbf{C}_i\Delta t,t)\right)+\mathcal{O}(\Delta t^2), \tag{8.3}$$

$$\Delta G=\frac{2}{T_0(\Delta t)^2}\left(\sum W_iG(\mathbf{x}+\mathbf{C}_i\Delta t,t)-G(\mathbf{x},t)\right)+\mathcal{O}(\Delta t^2). \tag{8.4}$$

For evaluation of g^{eq} in Eq. (8.1), we use entropic (isothermal) equilibrium given by

$$f_i^{\mathrm{eq}}(\rho,u_\alpha)=\rho W_i\prod_{j=1}^{D}\left[\left(2-\sqrt{1+\frac{u_j^2}{T_0}}\right)\left\{\frac{\left(2\frac{u_j}{C}+\sqrt{1+\frac{u_j^2}{T_0}}\right)}{1-\frac{u_j}{C}}\right\}^{C_{ij}/C}\right]. \tag{8.5}$$

Initial conditions are uniform density with random perturbation similar to 1D case. On time marching, we find that for temperatures below critical temperature, there is phase separation and condensing bubbles are formed. During the time evolution, bubbles merge and lead to a final state that is lamellar, cylindrical or a single spherical bubble (as shown in Fig. 5) based on the initial density.

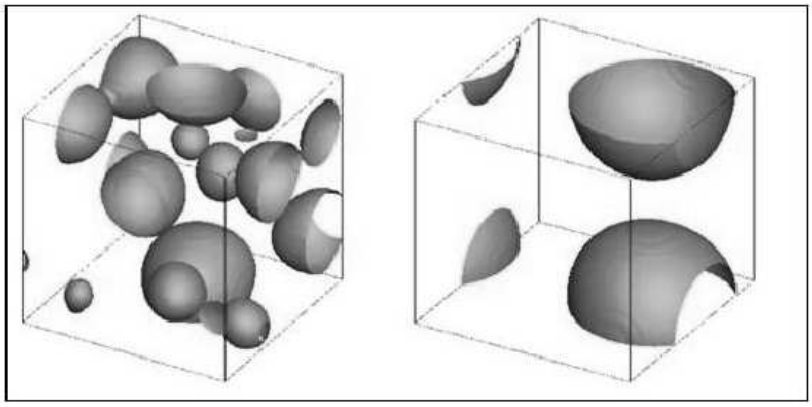

Figure 5: Evolution of iso density contours in D3Q27 simulation of a condensing bubble.

The comparison of observed final density ratios for different T/T_c is shown in Fig. 6. It can be seen that there is excellent agreement with theory and density ratios as high as 20 are achieved. The 3D setup is also more stable than 1D for high density ratios.

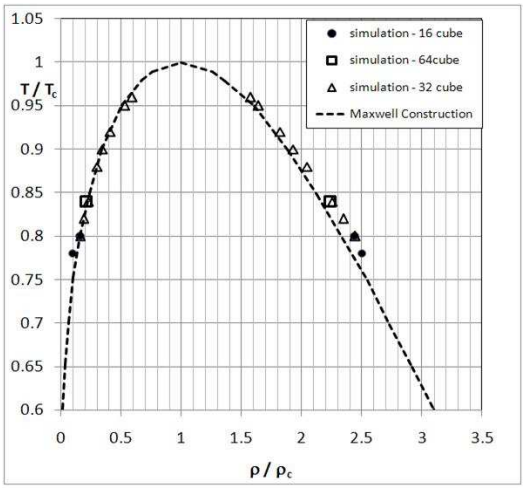

Figure 6: Comparison of observed liquid and gas densities in D3Q27 simulations with Maxwell construction for C-S EOS.

9 Outlook

The proposed extension to BGK-Boltzmann equation for dense gases by generalization of the propagation velocity has been assessed by comparison with MD. The Gibbs-Duhem relation has been exploited to obtain better discretization. The density dependence of viscosity has been accounted for and is seen to be important for stability of the scheme.

The numerical scheme developed has been successful in simulating condensation in a 3D periodic domain. While the existence of a valid H-theorem may not be expected for the present discrete model, we would like to emphasize that it is based on a continuous model that has an H-theorem. We would like to once again remind the reader that, unlike in case of dilute gas LBM, where the continuous equation has an H-theorem, the existing dense gas models do not have an H-theorem even for the continuous equations. One may expect that the discrete model based on a continuous model that has an H-theorem might be more stable than ones based on continuous models without an H-theorem. The objective of this paper is to demonstrate a preliminary numerical implementation of the continuous model presented in [1] and it is planned to develop an entropic version of the discrete scheme in future.

The current numerics are stable up to a density ratio 20 and reproduce Maxwell construction, with a naïve construction. One of the issues of the present scheme is that the viscosity is from Enskog theory. Ideally viscosity as a function of density should be extracted from MD simulations. Further, it is planned to develop a scheme that includes rigorous Hermite expansion with higher order terms. Comparison of the performance of the present scheme with other Enskog-type models, particularly with a recently proposed formulation based on density functional approach [36] would be subject of future work.

Acknowledgments

Suryanarayanan would like to thank ICAM-I2CAM, 1 Shields Avenue, Davis, CA 95616 for travel support through NSF grant number DMR-0844115 for attending DSFD2012 where this work was presented. Ansumali would like to thank Department of Science and Technology (DST), India for providing computational resources via Ramanujan Fellowship grant. We would like to thank the two referees for their valuable suggestions that has led to a significant improvement of this manuscript.

Appendix A: H-theorem and comparison with Ihle and Kroll model

Let us consider a generic model of the form

$$\partial_t f + v_\alpha \partial_\alpha f = \Omega + \partial_\alpha(\chi A_\alpha), \tag{A.1}$$

where Ω is usual collision models for point particle (either in Boltzmann or BGK form). For any dense gas model we would expect the entropy functional to be of the form given as [1],

$$H(\mathbf{x},t) = H^{\mathrm{ID}} - s^{\mathrm{nid}}(\rho(\mathbf{x},t)), \tag{A.2}$$

where s^{nid} is the excess entropy, known from equation of state, and ideal part is the usual Boltzmann H-function

$$H^{\text{ID}} = \int d\mathbf{v} f(\ln f - 1). \tag{A.3}$$

In order to construct evolution equation for such a quantity we multiply general kinetic equation with $\ln f$ and integrate over velocity space to obtain

$$\partial_t H^{\text{ID}} + \partial_\alpha J^{\text{ID}}_{H\alpha} = \int d\mathbf{v} \ln f \Omega + \int d\mathbf{v} \ln f \partial_\alpha (\chi A_\alpha), \tag{A.4}$$

where

$$J^{\text{ID}}_{H\alpha} = \int d\mathbf{v} v_\alpha f(\ln f - 1). \tag{A.5}$$

Eq. (A.4) can be simplified as

$$\partial_t H^{\text{ID}} + \partial_\alpha \left(J^{\text{ID}}_{H\alpha} - \chi A_\alpha \ln f \right) = \int d\mathbf{v} \ln f \Omega - \int d\mathbf{v} \chi A_\alpha \frac{1}{f} \partial_\alpha f. \tag{A.6}$$

Similarly, the evolution equation for the non-ideal part of the entropy can be written as

$$\partial_t s^{\text{nid}} + \partial_\alpha \left(u_\alpha s^{\text{nid}} \right) = \partial_\alpha \left(u_\alpha s^{\text{nid}} \right) - \frac{\delta s^{\text{nid}}}{\delta \rho} (u_\alpha \partial_\alpha \rho + \rho \partial_\alpha u_\alpha), \tag{A.7}$$

which can be simplified further, by noting that $\rho\chi = \left(s^{\text{nid}} - \rho \frac{\partial s^{\text{nid}}}{\partial \rho} \right)$ as

$$\partial_t s^{nid} + \partial_\alpha \left(u_\alpha s^{\text{nid}} \right) = \chi \rho \partial_\alpha u_\alpha, \tag{A.8}$$

which allow us to write the entropy evolution equation as

$$\partial_t H + \partial_\alpha J^H_\alpha = \int \Omega \log(f) d\mathbf{v} - \int d\mathbf{v} \chi B_\alpha \frac{1}{f} \partial_\alpha f, \tag{A.9}$$

where A_α is written as

$$A_\alpha = -(v_\alpha - u_\alpha) f + B_\alpha, \tag{A.10}$$

and entropy flux is defined as

$$J^H_\alpha = -s^{nid} u_\alpha + \int d\mathbf{v} f(\log f - 1) \hat{v_\alpha}. \tag{A.11}$$

The RHS of Eq. (A.9) should be negative for H-theorem to be satisfied. We know that this is always the case for the BGK-collision term. In the present model, $B_\alpha = 0$, hence H-theorem exists. But in the model of Ihle and Kroll [17]

$$B_\alpha = T \frac{\partial \pi}{\partial v_\alpha} + (v_\alpha - u_\alpha) f, \tag{A.12}$$

where π is a secondary distribution used for non-ideal part of the pressure and is approximately equals to equilibrium distribution $\pi \approx f^{\text{eq}}$. Further, using the approximate value for the first term in the above equation suggested in Eq. (32) of Ihle and Kroll [17]

$$B_\alpha = -(v_\alpha - u_\alpha) f^{\text{eq}} + (v_\alpha - u_\alpha) f. \tag{A.13}$$

This would imply that the only difference is the use of f^{eq} as against f in the present model. We can analyse the consequence of this seeming minor difference in context of hydrodynamics and H-theorem. The difference in hydrodynamic equations can be analyzed by computing lower order moment of this term, which is

$$\int dv B_\alpha = 0, \qquad \int dv B_\alpha v_\beta = \sigma_{\alpha\beta}, \tag{A.14}$$

where kinetic component of the stress tensor $\sigma^{(\text{K})}_{\alpha\beta}$ is defined in terms of $P^{(\text{K})}_{\alpha\beta} = \int f v_\alpha v_\beta d\mathbf{v}$ as

$$\sigma_{\alpha\beta} = P^{(\text{K})}_{\alpha\beta} - \rho u_\alpha u_\beta - \rho T \delta_{\alpha\beta}. \tag{A.15}$$

This implies that only higher order terms in the Hermite expansion of B_α are non-zero. Hence the hydrodynamics of both models are very similar. Thus, it can be said that though motivated from slightly different physical picture, present model and Ihle and Kroll model leads to very similar hydrodynamics. However, while in present case H-theorem can be proven (as $B_\alpha = 0$ in Eq. (A.9)), it is not obvious in the Ihle and Kroll model both for general case π as well as special case (where π is set equals to the equilibrium distribution). We would like to further note that this is only a very rough comparison as the Ihle and Kroll model involves more than one distribution function, and it is not even clear how to define an appropriate Lyapunov function for models with more than one distribution function.

Appendix B: Chapman-Enskog expansion for discrete model

The discrete scheme for the present model (based on non-ideal pressure) is given by

$$g(\mathbf{x} + \mathbf{C_i}\Delta t, t + \Delta t) = g(\mathbf{x}, t) + 2\beta \left(g_i^{\text{eq}}(\rho, \hat{\mathbf{j}}) - g_i \right) - 2\beta\tau \Delta^c_\alpha (W_i C_{i\alpha} \chi \rho), \tag{B.1}$$

where Δ^c stands for central difference operator and we have defined following conserved moments of the discrete populations

$$\sum_i g_i = \rho, \qquad \sum_i g_i C_{i\alpha} = j_\alpha \equiv \rho u_\alpha. \tag{B.2}$$

The momentum density appearing in the equilibrium expression is taken to be

$$\hat{j}_\alpha = j_\alpha - \frac{\Delta t}{2} \partial_\alpha (\chi \rho T_0). \tag{B.3}$$

Now onwards we set

$$\chi = \chi^{\mathrm{h}} + \chi^{\mathrm{Att}} \tag{B.4}$$

to denote the total chemical potential where the hard sphere and the attractive contribution are denoted by superscript h and Att respectively. Note that χ^{Att} is related to μ^{Att} by Gibbs-Duhem relation.

On Taylor expanding the above equation in space and time, we get

$$\begin{aligned}&\left[(\partial_t + C_{i\alpha}\partial_\alpha) + \frac{\Delta t}{2}(\partial_t + C_{i\alpha}\partial_\alpha)^2) + \cdots\right] g_i \\ =&2\frac{\beta}{\Delta t}\left(g_i^{\mathrm{eq}}(\rho, \hat{\mathbf{j}}) - g_i\right) - 2\beta\frac{\tau}{\Delta t}\partial_\alpha(W_i C_{i\alpha}\chi\rho) - 2\beta\tau\frac{(C\Delta t)^2}{3!\Delta t}[\partial_\alpha\partial_\beta\partial_\gamma(\delta_{\alpha\beta\gamma\theta}W_i C_{i\theta}\chi\rho)].\end{aligned} \tag{B.5}$$

In order to find out the hydrodynamic equation being simulated by the discrete model, we define a few higher order moments as

$$\sum_i g_i C_{i\alpha}C_{i\beta} = P_{\alpha\beta}, \qquad \sum_i g_i C_{i\alpha}C_{i\beta}C_{i\gamma} = Q_{\alpha\beta\gamma}, \qquad \sum_i g_i C_{i\alpha}C_{i\beta}C_{i\gamma}C_{i\theta} = R_{\alpha\beta\gamma\theta}. \tag{B.6}$$

We can find the evolution equation for the conserved quantities from the Eq. (B.5) as

$$\left(1 + \frac{\Delta t}{2}\partial_t\right)(\partial_t\rho + \partial_\alpha j_\alpha) + \frac{\Delta t}{2}\partial_\alpha\left(\partial_t j_\alpha + \partial_\beta P_{\alpha\beta}\right) = 0, \tag{B.7a}$$

$$\begin{aligned}&\left(1 + \frac{\Delta t}{2}\partial_t\right)\left(\partial_t j_\alpha + \partial_\beta P_{\alpha\beta}\right) + \frac{\Delta t}{2}\partial_\beta\left(\partial_t P_{\alpha\beta} + \partial_\gamma Q_{\alpha\beta\gamma}\right) \\ &\qquad = -\partial_\alpha(\chi\rho T_0) - 2\beta\tau\frac{(C^2\Delta t)}{3!}[\partial_\beta\partial_\gamma\partial_\theta(\delta_{\beta\gamma\theta\alpha}\rho\chi T_0)].\end{aligned} \tag{B.7b}$$

While, the kinetic part of the stress tensor evolves as

$$\begin{aligned}&\left(1 + \frac{\Delta t}{2}\partial_t\right)\left(\partial_t P_{\alpha\beta} + \partial_\gamma Q_{\alpha\beta\gamma}\right) + \frac{\Delta t}{2}\partial_\gamma\left(\partial_t Q_{\alpha\beta\gamma} + \partial_\theta R_{\alpha\beta\gamma\theta}\right) \\ =&\frac{2\beta}{\Delta t}\left[\left(\frac{\hat{j}_\alpha\hat{j}_\beta}{\rho}\right) + \rho T_0\delta_{\alpha\beta} - P_{\alpha\beta}\right].\end{aligned} \tag{B.8}$$

Now, expanding the spatial and time derivatives in terms of the smallness parameter ϵ (this would physically imply the smallness of Δt) as

$$\partial_t = \epsilon\partial_t^{(1)} + \epsilon^2\partial_t^{(2)}, \tag{B.9}$$

$$\partial_\alpha = \epsilon\partial_\alpha. \tag{B.10}$$

The coefficient of ϵ and in the mass density and the momentum density,

$$\partial_t^{(1)}\rho + \partial_\alpha j_\alpha = 0, \tag{B.11a}$$

$$\partial_t^{(1)} j_\alpha + \partial_\beta P^0_{\alpha\beta} = -\partial_\alpha(\chi\rho T_0). \tag{B.11b}$$

And, the coefficient of ϵ^2 in the mass density and the momentum density,

$$\partial_t^{(2)}\rho = -\frac{\Delta t}{2}\partial_t^{(1)}\left(\partial_t^{(1)}\rho + \partial_\alpha j_\alpha\right) - \frac{\Delta t}{2}\partial_\alpha\left(\partial_t^{(1)} j_\alpha + \partial_\beta P^0_{\alpha\beta}\right), \tag{B.12a}$$

$$\partial_t^{(2)} j_\alpha + \partial_\beta P^1_{\alpha\beta} = -\frac{\Delta t}{2}\partial_t^{(1)}\left(\partial_t^{(1)} j_\alpha + \partial_\beta P^0_{\alpha\beta}\right) - \frac{\Delta t}{2}\partial_\beta\left(\partial_t^{(1)} P^0_{\alpha\beta} + \partial_\gamma Q^0_{\alpha\beta\gamma}\right), \tag{B.12b}$$

where

$$P^0_{\alpha\beta} = \rho\hat{u}_\alpha\hat{u}_\beta + \rho T_0\delta_{\alpha\beta}, \qquad Q^0_{\alpha\beta\gamma} = \rho\hat{u}_\alpha T_0\delta_{\beta\gamma} + \rho\hat{u}_\beta T_0\delta_{\alpha\gamma} + \rho\hat{u}_\gamma T_0\delta_{\alpha\beta} + \mathcal{O}(\mathbf{u}^3). \tag{B.13}$$

Using evolution equation for kinetic part of the stress tensor at order of ϵ, we have

$$P^1_{\alpha\beta} = \frac{-\Delta t}{2\beta}[\partial_t^{(1)} P^0_{\alpha\beta} + \partial_\gamma Q^0_{\alpha\beta\gamma}]. \tag{B.14}$$

Using Eqs. (B.9) and (B.10), we get continuity equation as

$$\partial_t\rho + \partial_\alpha\hat{j}_\alpha = 0, \tag{B.15}$$

and the momentum equation as

$$\begin{aligned}\partial_t\hat{j}_\alpha + \partial_\beta\left(\frac{\hat{j}_\alpha\hat{j}_\beta}{\rho} + \underbrace{(1+\chi)\rho T_0}_{p}\delta_{\alpha\beta}\right) &= \partial_\beta[\underbrace{\rho T_0\tau}_{\eta_{\text{shear}}}\{(\partial_\alpha\hat{u}_\beta + \partial_\beta\hat{u}_\alpha) - \frac{2}{\mathrm{D}}\delta_{\alpha\beta}\partial_\gamma u_\gamma\}] \\ &+ \partial_\beta[\underbrace{\frac{2}{\mathrm{D}}\rho T_0\tau}_{\eta_{\text{bulk}}}\delta_{\alpha\beta}\partial_\gamma u_\gamma] - \underbrace{\tau\left(\hat{u}_\alpha\partial_\beta(\rho\chi T_0) + \hat{u}_\beta\partial_\alpha(\rho\chi T_0)\right)}_{\text{Galilean invariance violation}},\end{aligned} \tag{B.16}$$

where D is the dimension. The loss of Galilean invariance occurs due to the neglected term in Eq. (6.8). Further, the neglecting of this term also leads to the effective (bulk and shear) viscosity being reduced by a factor of $(1+\chi)$. We would like to note that these errors occur only at the Navier Stokes level. However, since the objective of the present work was to provide a numerical demonstration of phase transition based on the model proposed by [1] using a simple implementation, addressing this issue is left for future work.

References

[1] S. Ansumali. Mean-field Model beyond Boltzmann-Enskog Picture for Dense gases. Communications in Computational Physics, 9(5):1117–1127, 2011.

[2] S. Ansumali, I.V. Karlin, S. Arcidiacono, A. Abbas, and N.I. Prasianakis. Hydrodynamics beyond Navier-Stokes: Exact solution to the lattice Boltzmann hierarchy. Physical Review Letters, 98(12):124502, 2007.

[3] S.H. Kim, H. Pitsch, and I.D. Boyd. Slip velocity and Knudsen layer in the lattice Boltzmann method for microscale flows. Physical Review E, 77(2):026704, 2008.
[4] S.H. Kim and H. Pitsch. Analytic solution for a higher-order lattice Boltzmann method: Slip velocity and Knudsen layer. Physical Review E, 78(1):016702, 2008.
[5] W.P. Yudistiawan, S. Ansumali, and I.V. Karlin. Hydrodynamics beyond Navier-Stokes: The slip flow model. Physical Review E, 78(1):016705, 2008.
[6] F. Toschi and S. Succi. Lattice Boltzmann method at finite Knudsen numbers. EPL (Europhysics Letters), 69:549, 2005.
[7] V. Sofonea and R.F. Sekerka. Boundary conditions for the upwind finite difference lattice Boltzmann model: Evidence of slip velocity in micro-channel flow. Journal of Computational Physics, 207(2):639–659, 2005.
[8] Y.H. Zhang, X.J. Gu, R.W. Barber, and D.R. Emerson. Capturing Knudsen layer phenomena using a lattice Boltzmann model. Physical Review E, 74(4):046704, 2006.
[9] P.L. Bhatnagar, E.P. Gross, and M. Krook. A model for collision processes in gases. I. Small amplitude processes in charged and neutral one-component systems. Physical Review, 94(3):511, 1954.
[10] F.J. Higuera, S. Succi, and R. Benzi. Lattice gas dynamics with enhanced collisions. EPL (Europhysics Letters), 9:345, 1989.
[11] H. Chen, S. Chen, and W.H. Matthaeus. Recovery of the Navier-Stokes equations using a lattice-gas Boltzmann method. Physical Review A, 45(8):5339–5342, 1992.
[12] Y.H. Qian, D. d'Humieres, and P. Lallemand. Lattice BGK models for navier-stokes equation. EPL (Europhysics Letters), 17:479, 1992.
[13] X. Shan and H. Chen. Lattice Boltzmann model for simulating flows with multiple phases and components. Physical Review E, 47(3):1815, 1993.
[14] M.R. Swift, E. Orlandini, W.R. Osborn, and J.M. Yeomans. Lattice Boltzmann simulations of liquid-gas and binary fluid systems. Physical Review E, 54(5):5041, 1996.
[15] X. He and G.D. Doolen. Thermodynamic foundations of kinetic theory and lattice Boltzmann models for multiphase flows. Journal of Statistical Physics, 107(1):309–328, 2002.
[16] L.-S. Luo. Theory of the lattice Boltzmann method: Lattice Boltzmann models for nonideal gases. Phys. Rev. E, 62:4982–4996, 2000.
[17] T. Ihle and D.M. Kroll. Thermal lattice-Boltzmann method for non-ideal gases with potential energy. Computer Physics Communications, 129(1):1–12, 2000.
[18] S. Chapman and T.G. Cowling. The Mathematical theory of non-uniform gases. The Mathematical Theory of Non-uniform Gases, by Sydney Chapman and TG Cowling and Foreword by C. Cercignani, pp. 447. ISBN 052140844X. Cambridge, UK: Cambridge University Press, January 1991, 1, 1991.
[19] J.W. Dufty, A. Santos, and J.J. Brey. Practical Kinetic Model for Hard Sphere Dynamics. Phys. Rev. Lett., 77:1270–1273, 1996.
[20] J.F. Lutsko. Approximate Solution of the Enskog Equation far from Equilibrium. Phys. Rev. Lett., 78:243–246, 1997.
[21] L.-S. Luo. Unified Theory of lattice Boltzmann Models for Nonideal Gases. Phys. Rev. Lett., 81:1618–1621, 1998.
[22] X. Shan and H. Chen. Simulation of nonideal gases and liquid-gas phase transitions by the lattice Boltzmann equation. Physical Review E, 49(4):2941, 1994.
[23] J.W. Dufty, A. Santos, J.J. Brey, and R.F. Rodriguez. Model for nonequilibrium computer simulation methods. Phys. Rev. A, 33:459–466, 1986.
[24] A.W. Lees and S.F. Edwards. The computer study of transport processes under extreme

conditions. Journal of Physics C: Solid State Physics, 5:1921, 1972.
[25] N.F. Carnahan and K.E. Starling. Equation of state for nonattracting rigid spheres. The Journal of Chemical Physics, 51:635, 1969.
[26] J.F. Lutsko. Viscoelastic effects from the Enskog equation for uniform shear flow. Phys. Rev. E, 58:434–446, 1998.
[27] X. He, X. Shan, and G.D. Doolen. Discrete Boltzmann equation model for nonideal gases. Physical Review E, 57(1):13–16, 1998.
[28] S. Bastea and J.L. Lebowitz. Spinodal decomposition in binary gases. Physical Review Letters, 78(18):3499–3502, 1997.
[29] E.S. Kikkinides, M.E. Kainourgiakis, A.G. Yiotis, and A.K. Stubos. Lattice Boltzmann method for Lennard-Jones fluids based on the gradient theory of interfaces. Phys. Rev. E, 82:056705, 2010.
[30] J.S. Rowlinson and B. Widom. Molecular Theory of Capillarity. Dover Pubns, 2002.
[31] D. Moroni, B. Rotenberg, J.P. Hansen, S. Succi, and S. Melchionna. Solving the Fokker-Planck kinetic equation on a lattice. Physical Review E, 73(6):066707, 2006.
[32] T. Lee and P.F. Fischer. Eliminating parasitic currents in the lattice Boltzmann equation method for nonideal gases. Phys. Rev. E, 74:046709, 2006.
[33] A.J. Wagner. The origin of spurious velocities in lattice Boltzmann. International Journal of Modern Physics B, 17:193–196, 2003.
[34] S.S. Chikatamarla and I.V. Karlin. Entropy and galilean invariance of lattice Boltzmann theories. Phys. Rev. Lett., 97:190601, 2006.
[35] S. Ansumali, I.V. Karlin, and H.C. Öttinger. Minimal entropic kinetic models for hydrodynamics. EPL (Europhysics Letters), 63:798, 2003.
[36] U.M.B. Marconi and S. Melchionna. Kinetic theory of correlated fluids: From dynamic density functional to lattice Boltzmann methods. The Journal of Chemical Physics, 131:014105, 2009.